Quantitative Analysis of Gas Hydrates Using Raman Spectroscopy

Junfeng Qin and Werner F. Kuhs
GZG, Abteilung Kristallographie, Universität Göttingen, Goldschmidtstrasse 1, 37077 Göttingen, Germany

DOI 10.1002/aic.13994
Published online February 22, 2013 in Wiley Online Library (wileyonlinelibrary.com)

A calibration protocol to quantify the compositional information of gas hydrates using Raman spectroscopy is proposed. Structure I pure CH_4-, CO_2- and C_2H_6-hydrates in their deuterated and hydrogenated forms with known cage occupancies were investigated by Raman spectroscopy. Raman scattering cross sections of CH_4 in the large and small cages were found to be very similar, but not identical. Some C_2H_6 bands of C_2H_6-hydrate were tentatively reassigned or newly reported and assigned. Our results show that the relative cross sections of guest vibrational modes in the deuterated hydrate are in agreement with those in the hydrogenated hydrate, whereas they are considerably different from those in fluid phase. Using our Raman quantification factors, the relative cage occupancies can now be determined more reliably in CH_4-hydrates. Moreover, with additional assumptions, the absolute cage occupancies, the bulk guest composition and hydration number of pure or mixed gas hydrates become accessible by Raman spectroscopy. © 2013 American Institute of Chemical Engineers *AIChE J*, 59: 2155–2167, 2013

Keywords: Raman spectroscopy, gas hydrate, methane, carbon dioxide, ethane, quantification factor, cross section, hydration number

Introduction

Gas hydrates are nonstoichiometric crystalline solids containing guest molecules within host cages of H-bonded water molecules.[1] Naturally occurring gas hydrates are stable at relatively low temperature (typically < 285 K) and high pressure (typically >2 MPa) conditions, and occur frequently in and below continental permafrost as well as in marine environments of continental margins.[2] The encaged guest molecules interact with the hydrate lattices via van der Waals interactions; the main guest constituent is CH_4 with additions of higher hydrocarbons like C_2H_6, as well as CO_2, N_2 and H_2S. Depending on temperature, pressure, molecular size and guest composition, three common structures are identified: which correspond to different frameworks of water molecules; they are referred to as cubic sI, cubic sII and hexagonal sH. The sI structure is considered to be the most common hydrate structure and comprises two small 5^{12} (SC, for short) and six large $5^{12}6^2$ (LC) cages per unit cell, formed by 46 water molecules. The sII unit cell consists of 16 small 5^{12} and eight large $5^{12}6^4$ cages formed by 136 water molecules, and the sH unit cell contains three small 5^{12}, two medium $4^3 5^6 6^3$ and one large $5^{12}6^8$ cages formed by 34 water molecules. For a pure hydrate with only one type of small guest molecule like CH_4, C_2H_6 and CO_2, sI hydrate is usually formed at moderate pressures.[3–6] sII hydrates were observed to coexist metastably with sI CH_4- and CO_2-hydrates.[7–9] For a mixed hydrate with two or more types of guests, like a CH_4-C_2H_6 mixture, the hydrate structure may vary with the different composition and/or prevailing P-T conditions.[10–13] CH_4, CO_2 and C_2H_6 occupy both the small and large cages. Being in competition for the SCs and LCs, CO_2 and C_2H_6 partition more favorably into the LCs, while CH_4 fills the SCs.[11,14,15] Furthermore, large cages are generally almost fully occupied, whereas the occupancy of small cages varies by guest.[1]

Natural gas and oil industries have been interested in hydrate research since the 1930s as a consequence of the unwanted hydrate formation in pipelines leading to their complete blockage.[1] This interest has increased recently because of several factors. First, the total amount of hydrate-bound methane in geological deposits is large enough to be of possible interest as a future energy resource, although estimations vary by several-orders of magnitude.[16–18] Second, since global warming destabilizes continental gas hydrates, liberating the very active greenhouse gas methane, may lead to a considerable positive feedback.[19] Third, realizing that CO_2-hydrate is thermodynamically more stable than CH_4-hydrate, a reduction of the anthropogenic greenhouse gas CO_2 via the storage as solid CO_2-hydrate in a sedimentary gas hydrate reservoir was proposed, while simultaneously recovering hydrocarbons.[20–22] This technique with a maximum of 64% replacement achieved in a CO_2-CH_4 system without additional constituents could help to resolve environmental issues while recovering a primary source of energy.[14] To apply this idea to a larger scale, a better understanding of the involved gas hydrate formation and dissociation mechanisms is required.

Raman spectroscopy, a nondestructive technique, is one of the most powerful tools to investigate both synthetic and

Correspondence concerning this article should be addressed to W. F. Kuhs at wkuhs1@gwdg.de.

natural hydrates at the molecular level.[23–27] One important feature of confocal Raman spectroscopy is the capability to sample small area with a diameter of a few microns, providing information on the homogeneity of gas hydrates by looking at the individual gas hydrate particles.[28] In contrast, nuclear magnetic resonance (NMR) spectroscopy,[29–31] neutron and X-ray powder diffraction (NPD and XRPD, respectively)[32–34] usually provide bulk information; the spatial resolution of nuclear magnetic resonance imaging and synchrotron microdiffraction is typically one to two orders of magnitude lower than what is routinely available for confocal Raman spectroscopy. In addition, it is simpler and easier to be accessed, compared with neutron or synchrotron diffraction[35] and NMR.[23,29]

Raman spectroscopy is routinely used in a qualitative analysis of gas hydrates, such as their chemical and structural identification. The vibrational modes of the guests (in terms of position, full width at half maximum (FWHM) and peak area) depend on the local environment of the hosting cages and can often be used to identify structure type and cage preferences. The pioneering Raman spectroscopic work was performed by Anthonsen[36] on some halogen gas hydrates in 1974. He found the interactions between guest molecules and the hydrate lattice to be very weak when comparing Raman spectra of guests in gas phase and in hydrate cavities. CH_4-CO_2-H_2O sI hydrates synthesized from CH_4-CO_2-H_2O mixtures forming fluid inclusion in quartz were investigated by Seitz et al.[37] They came to two conclusions based on their Raman spectra of CH_4-CO_2-H_2O sI hydrate which were later found to be wrong (1) the assignments of the splitting Raman bands at 2903.5 and 2913 cm^{-1} as the C—H stretching-mode of CH_4 in SCs and LCs, respectively, (2) the suggestion of CO_2 only occupying the large cages in view of the nondoubling of the Fermi dyad of CO_2. Nakahara et al.[38] reported Raman investigation of natural air hydrate containing N_2 and O_2, found in deeper parts of polar ice cores. The composition ratio of N_2-O_2 was determined from the peak areas of their vibrational modes; the peak positions were found to downshift as temperature becomes lower. Assuming that Raman intensities of both H_2O and CO_2 are proportional to their molar fractions, Uchida et al.[39] determined for the first time the hydration number (i.e., the number of water molecules per guest atom) of CO_2-hydrate by comparing Raman intensities of H_2O and CO_2 molecules of CO_2-hydrate with those of a CO_2-saturated water solution. Sum et al.[23] reassigned the two distinct Raman lines of CH_4 sI hydrate and systematically studied the applications of Raman for determining structure type, cage occupancies and bulk composition of gas hydrates. The intensity-wise counterintuitive assignment of Raman frequencies to the large and small cages[37] were resolved by Subramanian and Sloan[15] by referring to the "loose cage-tight cage" model proposed by Pimentel and Charles.[40] More recently, *in situ* or time-resolved Raman spectroscopy has provided access to study processes in gas hydrates, such as structural transitions, as well as their formation and dissociation kinetics.[22,41]

Compositional information, i.e., type and proportion of guest species, the cage occupancies of the various guests and the hydration number, is of primary importance for understanding the physical and physicochemical properties of gas hydrates. ^{13}C solid-state NMR is considered as a reliable quantitative method and has been applied to interpret the relative cage occupancies of guest molecules in gas hydrates including CH_4, C_2H_6 and CO_2.[29–31,42] XRPD is mostly used to provide information on the structure type and unit cell parameters of gas hydrates; efforts were made to determine the absolute cage occupancies of pure gas hydrates by direct-space methods based on laboratory XRPD[43] or by using high-resolution synchrotron XRPD[34]; this was previously only possible using single crystals, which are not easily available and also not easily handled in the case of gas hydrates. Raman spectroscopy does not directly provide the absolute cage occupancies—at least not without further thermodynamic assumptions.[24] Relative cage occupancies, however, can be established straightforwardly: for sI CH_4-hydrate the relative cage occupancies of methane in the LCs and SCs deduced from Raman spectroscopy, obtained under the tacit assumption of identical cross section for CH_4 in both cages, are found to be in reasonable agreement with NMR-results.[44,45] The results for mixed hydrates are more doubtful as evidenced in the following two publications: Kumar et al.[33] found that the compositional information of sII CH_4-C_2H_6-C_3H_8 hydrate determined by ^{13}C magic angle spinning NMR spectroscopy is in agreement with the one obtained from Raman spectroscopy and gas chromatography. In contrast, Wilson et al.[44] cross-calibrated the cage occupancy ratio of CH_4-CO_2 sI hydrate by Raman and ^{13}C NMR spectroscopy and found that the difference was approximately 12% for the one reported sample. A further direct comparison between Raman and NMR or XRPD for the mixed hydrate containing CH_4 and CO_2 molecules appears to be necessary. It appears that Raman spectroscopy cannot be applied to accurately quantify the composition of a mixed hydrate without being calibrated by other techniques; in particular, the Raman cross sections of guests in different environments need to be established quantitatively. This indeed has been attempted by geochemists, which have established Raman spectroscopy as a powerful stand-alone quantification method to determine the bulk composition of gases, such as CH_4, CO_2, N_2, and gas-water mixture in fluid inclusions[37,46–50] and it is certainly worth considering this large body of work.

Quantitative Raman analysis

The quantitative analysis of Raman spectroscopy is based on Placzek's polarizability theory[46,51] as given by

$$A_i = I_0 \sigma_i N_i \eta_i \tag{1}$$

where A_i is the integrated peak area (intensity) of a Raman active peak for the species i over a finite range, I_0 is the irradiance on the sample, σ_i is the Raman scattering cross section of i at a certain wavelength of the exciting source, N_i is the number of molecules of i in the irradiated volume, η_i is the instrumental efficiency of the optical and electronic response. Equation 1 relates the intensity of each species (A_i) to the number of molecules present in the scattering volume (N_i). Therefore, it is possible to determine the relative proportion of species by comparing their relative intensities. The molar fraction of a certain species a (x_a) can be derived from rearranging Eq. 1

$$x_a = [A_a/(\sigma_a \eta_a)] / \sum_{i=1}^{n} [A_i/(\sigma_i \eta_i)] \tag{2}$$

$$= [A_a/F_a] / \sum_{i=1}^{n} (A_i/F_i) \tag{3}$$

where F_a is the Raman quantification factor (F-factor) of species a, and i refers to all species in the mixture.

Obviously, the accurate determination of the composition of a mixture is possible only if σ and η or F values of all species in the system are accurately known. The Raman cross section is the instrument-independent Raman scattering efficiency representing the property of a molecule in the local environment; it is sensitive to pressure and composition.[48] To determine the guest composition, the combined factor F is more advantageous than an individual calibration of σ and η for a specific Raman spectrometer.[50] For a mixture, in the case that spectra of species in the same phase (for gas hydrate, it means structure type) and chamber are acquired at the same time or immediately one after the other, it is reasonable to assume that the instrumental efficiencies of different species are identical.[46] This is to say, the cross-section ratio of species a and b (σ_a/σ_b) is assumed to be equal to the relative F-factor (F_a/F_b). Seitz et al.[37] obtained the molar ratios of CH_4 to CO_2 in a variety of CH_4-CO_2-H_2O mixtures trapped into fluid inclusions using Raman spectroscopy and the results are comparable with the determination by microthermometry. Seitz et al.[49] investigated the relative Raman F-factor of CH_4 to CO_2 (F_M/F_C) in a CH_4-CO_2 mixture for a wide range of temperatures, pressures and compositions, and found that (1) the variation of F_C/F_M (namely, σ_C/σ_M) with composition is not significant within their analytical uncertainty, and (2) F_C/F_M in an equimolar mixture continuously increases with the increasing pressure up to 10 MPa. This may reflect that molecular interactions could indeed be significant in this pressure interval. They also reported that the relative quantification factors of CH_4 to CO_2 in binary CH_4-CO_2 and ternary CH_4-CO_2-H_2O systems are different.[37,49] Burke summarized the available σ values for dozens of gas species in fluid phase, and emphasized all these data were calibrated from low-density fluid mixtures.[48]

Considerable efforts have also been made to independently quantify guest compositions for gas hydrates by Raman spectroscopy.[10,13,22,23,38,52] Assuming the cross sections of species in fluid phase and in hydrate lattices being identical, Sum et al.[23] and Subramanian et al.[10] determined the composition of CH_4-CO_2- and CH_4-C_2H_6-hydrates by experimentally calibrating the ratios F_C/F_M and F_E/F_M in a variety of binary CH_4-CO_2 and CH_4-C_2H_6 mixtures in fluid phase under a certain pressure, respectively. However, they did not investigate the effect of pressure on the relative F-factors. Chazallon et al.[52] reported the molar proportions of N_2 and O_2 in the N_2-O_2 synthesis hydrate by using the available cross-section values published by Schrötter and Klöckner.[51] Ota et al.[22] directly took the value of the relative F-factor of CH_4 to CO_2 given by Sum et al.[23] to determine relative abundance of CH_4 after methane hydrate was replaced by liquid CO_2, although they were under different experimental conditions. The validity of the assumption of transferability of Raman cross section of gas in fluid phase to gas hydrate work remains doubtful, however. First, the chemical environment of guests in fluid phase and in hydrate lattices is apparently different, which may result in a significant difference in Raman scattering cross section. Second, the guest concentration in gas hydrate is very high, for example, 1 m^3 methane hydrate contains the same amount molecules as 164 m^3 methane at 293 K and 0.1 MPa,[1] and approximately 1 m^3 methane at 293 K and 13.2 MPa. Thus, due to the different densities, the relative F-factor of guests in fluid phase calibrated at one certain pressure cannot be used to determine the composition of gas hydrate without further calibration. Consequently, a quantitative interpretation of a Raman spectrum of a mixed gas hydrate requires the accurate knowledge of the relative quantification factors for each species in hydrate lattice.

In this article, we describe a calibration procedure to quantify the cage occupancies of guest, the bulk guest composition, as well as the hydrate number of gas hydrates using Raman spectroscopy. Peak positions, FWHMs and intensities of pure deuterated sI CO_2-, CH_4- and C_2H_6-hydrates and pure hydrogenated sI CO_2- and CH_4-hydrates were studied. New assignments were tentatively made for some ethane bands in sI C_2H_6-D_2O hydrates, based on the corresponding bands of ethane in fluid phase. Using Placzek's polarizability theory, the relative Raman quantitative factors of CO_2/CH_4, C_2H_6/CH_4, and guests to host molecules in hydrate lattices were experimentally determined by comparing the intensities of the specific Raman peaks of pure sI CO_2-, CH_4- and C_2H_6-hydrates with known composition obtained from synchrotron X-ray powder diffraction. With several assumptions, the empirical F-factors derived from pure sI gas hydrate can be applied for the mixed gas hydrates.

Experimental Methods

Sample preparation and X-ray diffraction

For the Raman calibration work 11 types of pure sI gas hydrates with known formation conditions, the cage occupancies and hydration number were used (see Table 1). The time-space averaged small (θ_S) and large (θ_L) cage occupancies, expressed as the percentage of the occupancy of a given cage with one guest molecule, for deuterated sI C_2H_6-hydrate were obtained by crystallographic Rietveld refinements of powder diffraction data obtained on the hard X-ray beamline BW5, HASYLAB at DESY, Hamburg;[34] the θ_S and θ_L cage occupancies of pure sI CO_2- and CH_4-hydrates were obtained from high-resolution powder diffraction data measured on ID31 at ESRF/Grenoble.[11,53] All cage occupancies together with their least-squares estimated standard deviations are given in Table 1. Considering the composition of sI, the hydration number (n) of sI gas hydrate was determined by

$$n = 46/(6\theta_L + 2\theta_S) \tag{4}$$

A detailed description of the hydrate synthesis and diffraction setups has been given in previous work.[7,34,53–55] Here, we only briefly summarize the procedures. All hydrate samples were synthesized in a custom-built high-pressure cell by exposing particles of H_2O or D_2O ice Ih to a specific gas at isobaric condition. The ice particles were obtained in an apparatus, in which H_2O or D_2O (purity given as 99.9%) water was sprayed into liquid N_2 to form spherical ice particles with a typical diameter of tens of μm. To prevent a contamination from atmospheric H_2O, D_2O ice was produced in a glovebox prepurged with N_2. Ice particles were collected into thin-walled Al-cans, and then placed into the pressure cell within a cryostat bath controlled at the desired temperature. Immediately after closing the pressure cell, gas was admitted up to the designated pressure. All pure CH_4 and CO_2 hydrates were formed under isothermal (close to the ice melting point) and isobaric condition, while the bath temperature for C_2H_6 hydrate was later increased above the ice melting point to allow for a more complete conversion of

Table 1. Synthesis Conditions, Cage Occupancies and Hydration Number Established by Synchrotron XRPD for the Gas Hydrates Used

Sample	P/MPa	T/K	D/day	θ_S/%	θ_L/%	n
CH_4-D_2O	3.5	271	21	85.8 ± 1.3[a]	99.6 ± 1.0[a]	5.99 ± 0.05[a]
CH_4-D_2O	6	271	21	85.6 ± 0.4[a]	98.9 ± 0.3[a]	6.02 ± 0.01[a]
CH_4-D_2O	10	271	21	87.3 ± 0.8[a]	100.0 ± 0.5[a]	5.94 ± 0.02[a]
CH_4-D_2O	15	271	21	88.5 ± 0.4[a]	100.0 ± 0.5[a]	5.93 ± 0.02[a]
CH_4-H_2O	3.5	268	21	85.6 ± 0.4[a]	98.3 ± 0.3[a]	6.05 ± 0.01[a]
CH_4-H_2O	6	268	21	87.1 ± 0.5[a]	100.0 ± 0.5[a]	5.95 ± 0.02[a]
CH_4-H_2O	10	268	21	87.0 ± 0.9[a]	100.0 ± 0.5[a]	5.95 ± 0.03[a]
CH_4-H_2O	15	268	21	85.4 ± 0.4[a]	100.0 ± 0.5[a]	5.97 ± 0.02[a]
CO_2-H_2O	3	268	21	68.5 ± 0.4[b]	98.4 ± 0.3[b]	6.33 ± 0.02[b]
CO_2-D_2O	3	271	21	67.4 ± 0.3[b]	98.9 ± 0.1[b]	6.32 ± 0.01[b]
C_2H_6-D_2O	3.8	270[d]	7[d]	–	–	–
		278[e]	14[e]	4.8[c]	100[c]	7.55[c]

[a]Cage occupancies are the unpublished values given by Hartmann.
[b]Data are taken from Hartmann et al.[53]
[c]Data are taken from Murshed et al.[34]
[d]and [e] correspond to the two stages at different temperatures and durations to form sI C_2H_6-D_2O hydrate.

ice particles into gas hydrates; for details see Table 1. The hydrate formation reactions were allowed to proceed typically for several weeks. The reaction was stopped by rapid cooling while concomitantly releasing the pressure, the samples recovered within seconds and transferred to a liquid nitrogen Dewar, where they were stored for subsequent use. Samples for Raman measurements were grinded into a size of 200–300 μm, and also stored under liquid N_2.

Apparatus

Raman spectra were acquired by a confocal Raman spectrometer (LabRAM HR800, Horiba Jobin Yvon) equipped with a 600 grooves/mm grating and a Peltier-cooled charge-coupled device detector (DU 420A, Andor, 1024 × 256 pixels). An Ar^+ laser (Innova 9C, Coherent) emitting a wavelength of 488 nm was used as the excitation source at the output power of 20.5 mW. Measurements were made in confocal configuration by focusing the laser beam via 50× long working distance objective (Numerical aperture = 0.55, Olympus). The backscattered mode was used. The confocal aperture was set to 100 μm. The resulting diameter and the power of laser beam on the focused sample were around 1.1 μm and 4.5 mW, respectively. Each spectrum, collected at a nominal resolution of 2.2 cm^{-1}, was obtained in two accumulations of 30 s exposure time within a range of 100 cm^{-1} to 4000 cm^{-1}. The temperature of the Raman laboratory was controlled to 295 ± 1 K by an air-conditioner.

The Raman analysis was carried out in a cooling and heating stage (Linkam THMS600), which was placed under an Olympus microscope attached to the spectrometer. The device was operated at 113 K with an ambient pressure N_2 atmosphere to prevent gas hydrate decomposition. The precision of the temperature control as well as the stability of temperature during the measurements was ±0.1 K. To calibrate the Raman quantification factors, pure deutereated sI CO_2-, CH_4- and C_2H_6-hydrates were loaded into three separate areas of the cooling chamber; then the samples were measured one after the other. In the same way, pure hydrogenated sI CO_2- and CH_4-hydrates were studied. Three to four sets of spectra were recorded for each loading, and three loadings were made. The temporal interval between two consecutive Raman measurements of the separated samples of one loading was typically 4–6 min.

Because of a possible nonlinearity of the spectrometer, peak position was calibrated against three emission lines of a mercury lamp (in air) at 2179.30, 3159.61 and 3222.64 cm^{-1}. Emission lines were recorded simultaneously with the Raman spectra of samples, rather than measured before or after each sample measurement, as shown in Figure 1. In principle, this procedure allows for a better accuracy in determining the peak positions while simplifying the measurement procedures. The estimated uncertainty obtained from the reproducibility of peak position determined by this method is better than ±0.8 cm^{-1}. After the baseline correction, each spectrum was fitted in the region of interest by a Gaussian/Lorentzian mixed function using "dmfit" software.[56] The Gaussian/Lorentzian ratio y (yG/(1-y)L) was established for each peak and then kept constant during further analysis. Raman spectral parameters, such as peak position, FWHM and the integrated area, were determined.

Results and Discussion

Methane hydrate

CH_4-D_2O and CH_4-H_2O sI hydrates formed at 6 MPa were chosen for the investigation of the Raman peak positions and FWHMs, as listed in Table 2; the uncertainties as obtained from the reproducibility are shown. Four bands of CH_4 molecules encaged into the deuterated or hydrogenated

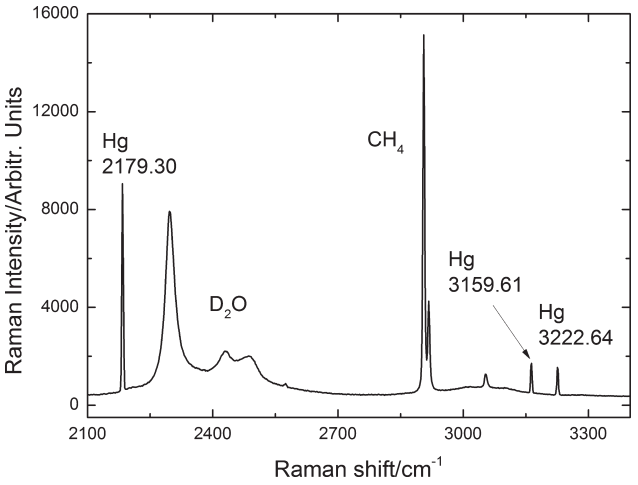

Figure 1. A representative Raman spectrum showing the bands of CH_4-D_2O hydrate and three emission lines of mercury recorded simultaneously.

Table 2. Assignments, Gaussian/Lorentzian Ratio *y* (*y*G/(1-*y*)L), Peak Positions and Full Width at Half Maximums (FWHMs) of Raman Bands of the Deuterated and Hydrogenated sI CH_4-Hydrates Formed at 6 MPa Measured at 113K under Atmospheric Pressure of N_2

			sI CH_4-D_2O hydrate		sI CH_4-H_2O hydrate	
Assign.	Cage	*y*	ν/cm^{-1}	FWHM/cm^{-1}	ν/cm^{-1}	FWHM/cm^{-1}
$2\nu_4$	–	0.0	2570.3 ± 0.5	4.8 ± 0.9	2569.8 ± 0.2	4.4 ± 0.5
ν_1	5^{12}	0.6	2901.6 ± 0.1	4.8 ± 0.3	2901.3 ± 0.2	5.0 ± 0.2
ν_1	$5^{12}6^2$	0.45	2913.4 ± 0.2	5.5 ± 0.3	2913.0 ± 0.1	6.3 ± 0.4
$2\nu_2$	–	0.0	3050.1 ± 0.2	7.5 ± 0.4	3048.9 ± 0.4	9.4 ± 0.5

sI hydrate were observed, as illustrated in Figure 2. Two strong distinct peaks at 2901.3 cm^{-1} and 2913.0 cm^{-1} are related to the totally symmetric C—H stretching mode (ν_1)[23] of CH_4 in the LCs and SCs of the hydrogenated framework, respectively, while the ν_1 bands arising from CH_4 trapped into the LCs and SCs of the deuterated hydrate lattices are located at 2901.6 and 2913.4 cm^{-1}, respectively. The widths of ν_1 bands of CH_4 in the hydrogen-bonded water cages are slightly bigger than those in the deuterated cages. Compared with the corresponding excitation obtained in the gas phase with only one band ≈ 2917.1 cm^{-1},[57] the band splits and both resulting bands are redshifted highlighting the change of the methane molecules' particular chemical environment. The published values for the ν_1 vibration of CH_4 given by different authors vary from 2901.2 to 2905 cm^{-1} for CH_4 in LC and from 2913.6 to 2916 cm^{-1} in SC of sI CH_4-hydrate.[11,23,25,58,59] The differences may be due to different temperatures and pressures during the data collection. The peak positions reported here are close to the values given by Ohno et al.[58] obtained at 95 K in a nitrogen atmosphere using laser light at a wavelength of 632.8 nm. Mangir and Kuhs[11] found that positions of the ν_1 bands of sI CH_4-hydrate shift to higher wave numbers by less than 1 cm^{-1} when temperature increases from 113 K to 173 K, however, no investigation has been made on the temperature dependence of the band positions of sI CH_4-hydrate at higher temperature. Moreover, Lu et al.[57] reported that Raman frequency of methane in vapor phase changes as a simple function of vapor density. It could imply that the ν_1 bands of CH_4 molecules in sI CH_4-hydrate also vary with the different cage occupancies. A broader band at 3048.9 and 3050.1 cm^{-1} is the overtone of C—H asymmetric bending mode ($2\nu_2$) of methane included in the hydrogenated and deuterated hydrate, respectively. It is approximately 3–4 cm^{-1} lower than the previous data.[11,27,60] Another minor peak at 2570.3 cm^{-1}, superimposed by the broad O—D stretching mode of D_2O framework, and at 2569.8 cm^{-1} is the first overtone of the C—H bending mode ($2\nu_4$) of CH_4 enclathrated in the deuterated and hydrogenated hydrate lattices, respectively. Chazallon et al.[27] gave the similar peak position of $2\nu_4$ band under the similar measurement conditions.

The cage occupancy ratio reflecting the distribution of CH_4 molecules in the large and small cages is generally determined by directly comparing peak areas of the two ν_1 bands of CH_4 included in sI hydrate lattices. In this study, the intensities of the C—H stretching mode of CH_4 enclathrated in the LCs and SCs of sI hydrogenated and deuteratated hydrates formed at different pressures, A_{ML} and A_{MS}, were integrated within the range of 2830–3000 cm^{-1}. As mentioned previously, for sI gas hydrates the number of the large cages is three times that of the small cages. The cage occupancy ratio of CH_4 can be obtained by

$$\theta_{ML}/\theta_{MS} = A_{ML}/3\sigma_{ML} \,/(A_{ML}/\sigma_{MS}) \quad (5)$$

$$\approx A_{ML}/3A_{MS} \quad (6)$$

where θ_{ML}, θ_{MS} and σ_{ML}, σ_{MS} are the absolute fractional occupancies and the Raman scattering cross sections of methane molecules in the large and small cages, respectively. Assuming σ_{ML} and σ_{MS} to be identical, Eq. 6 was used to determine cage occupancy ratio of CH_4 and the hydration number in sI methane hydrate.[23,24] However, the different cage sizes can be assumed to cause slightly different C—H bond lengths of CH_4 in the LCs and SCs; consequently, the Raman scattering cross sections of CH_4 in two cages can be expected to be somewhat different.[25,61]

To elucidate the possibly slightly different Raman scattering cross sections for CH_4 in small and large cages, the θ_{ML}/θ_{MS} ratios of deuterated and hydrogenated sI CH_4-hydrates, synthesized at different *P*-*T* conditions, were cross-calibrated by our synchrotron X-ray powder diffraction and Raman data obtained for the same samples. The cage fillings, established straightforwardly from diffraction data with a precision of typically better than 1% (see Table 1), together with a similar precision of the Raman intensity measurements allow us for the first time to proceed; the $\theta^R_{ML}/\theta^R_{MS}$ ratios were computed using Eq. 6 and are given in Table 3 with their standard deviations for the measured data. It can be seen that the ratios determined by synchrotron powder diffraction measurements $\theta^D_{ML}/\theta^D_{MS}$ are generally slightly higher than those from Raman spectroscopy $\theta^R_{ML}/\theta^R_{MS}$, but still comparable. Relying on the absolute values obtained from diffraction, the relative Raman scattering cross sections $\sigma^R_{ML}/\sigma^R_{MS}$ can be calculated using Eq. 5 with uncertainties

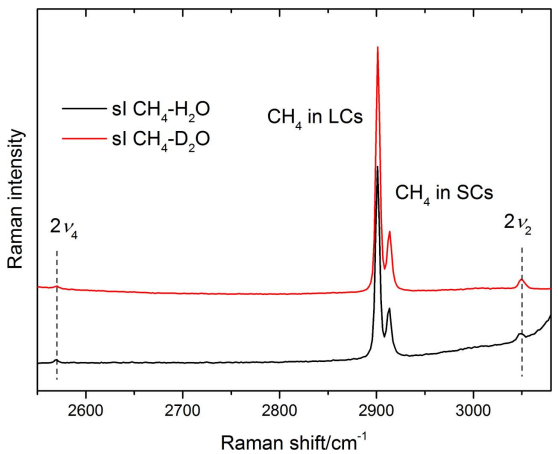

Figure 2. Typical Raman spectra of deuterated and hydrogenated sI CH_4-hydrates measured at ambient pressure and 113 K.

[Color figure can be viewed in the online issue, which is available at wileyonlinelibrary.com.]

Table 3. Relative Cage Occupancies and Raman Scattering Cross Sections of sI CH_4-D_2O and CH_4-H_2O Hydrate Determined by Synchrotron XRPD and Raman Measurements

Sample	T/K	P/MPa	$\theta^D_{ML}/\theta^D_{MS}$	$\theta^R_{ML}/\theta^R_{MS}$	$\sigma^R_{ML}/\sigma^R_{MS}$
CH_4-D_2O	271	3.5	1.16 ± 0.02	1.148 ± 0.014	0.989 ± 0.012
CH_4-D_2O	271	6	1.16 ± 0.01	1.125 ± 0.011	0.974 ± 0.009
CH_4-D_2O	271	10	1.15 ± 0.01	1.100 ± 0.023	0.960 ± 0.020
CH_4-D_2O	271	15	1.13 ± 0.01	1.077 ± 0.020	0.953 ± 0.019
CH_4-H_2O	268	3.5	1.15 ± 0.01	1.150 ± 0.017	1.002 ± 0.015
CH_4-H_2O	268	6	1.16 ± 0.03	1.135 ± 0.026	0.977 ± 0.022
CH_4-H_2O	268	10	1.15 ± 0.01	1.110 ± 0.024	0.965 ± 0.021
CH_4-H_2O	268	15	1.17 ± 0.01	1.102 ± 0.021	0.941 ± 0.018

[D] and [R] indicate diffraction and Raman methods, respectively.

obtained from error propagation. The relative cage occupancies derived from Raman scattering for both H_2O and D_2O hydrates appear to decrease as the synthesis pressure increases from 3.5 to 15 MPa; the reason for this behavior is not entirely clear, however, a possible explanation is a pressure-dependent (i.e., cage-filling dependent) change of the relative size of the SCs and LCs[62] with a corresponding slight change of relative cross section. As it can be seen from Table 3, the relative cross sections of CH_4 in the small and large cages for sI deuterated and hydrogenated hydrates formed under the same experimental conditions are not significantly different.

The average value of sI CH_4-H_2O and CH_4-D_2O hydrates formed at pressures from 3.5 to 15 MPa is 0.974 ± 0.028. The error is the standard deviation from the mean of totally 120 measurements. Undoubtedly, the Raman scattering cross section of CH_4 in $5^{12}6^2$ cages is close to that in 5^{12} cages, but they are not identical. It is the first time to experimentally confirm the difference of the Raman scattering cross sections of CH_4 encaged into the large and small cages of sI CH_4-hydrate predicted by Tulk.[25] Therefore, to obtain the accurate values predicted by Raman spectroscopy, such as the cage occupancy ratio, and with further thermodynamic assumptions,[23,24] the hydration number of sI CH_4-hydrate, the determined should be used as a correction factor.

Carbon dioxide hydrate

In Figure 3, one characteristic doublet, also known as Fermi dyad, was observed at 1277.6 and 1382.8 cm^{-1} for sI CO_2-D_2O hydrate, and 1275.5 and 1379.4 cm^{-1} for sI CO_2-H_2O hydrate. These two respective bands correspond to the lower (v_{c-}) and upper (v_{c+}) levels of Fermi resonance resulting from two vibrational modes with nearly the same energy: the symmetric stretching vibration v_1 and the overtone of the bending modes $2v_2$ of CO_2 molecules trapped into hydrate cavities. These two modes perturb each other in the exited states through Fermi resonance. The peak positions of Fermi bands in H_2O hydrate host are considerably lower than in the D_2O framework, see Table 4. In addition, the v_{c-} band of CO_2-D_2O hydrate is almost twice as broad as that of CO_2-H_2O hydrate. Our results of CO_2 bands in H_2O lattices are on the lower side of the published data, which vary in a range of 1274–1278 cm^{-1} and 1377–1384 cm^{-1}.[23,39,63,64] As discussed earlier, CO_2 molecules occupancy both the LCs and SCs,[42,65] but Raman bands of CO_2 between the LCs and SCs are overlapping and cannot be resolved in this study. A weaker peak around 1368.4 cm^{-1} for CO_2-D_2O hydrate and 1366.6 cm^{-1} for CO_2-H_2O hydrate is related to the isotopic splitting of $^{13}CO_2$ referring to the previous assignments for $^{13}CO_2$ in vapor phase.[66] The large uncertainty shows this peak is difficult to be resolved due to its weakness and overlap with the upper Fermi dyad.

Ethane hydrate

Raman spectra of C_2H_6 are more complex due to the molecules' six Raman-active fundamental modes, many overtones and combinations as described by Helvoort et al.[67] Raman spectra of the C—C and C—H stretching vibrations of ethane trapped into hydrate lattices have been studied to determine hydrate structure type and to estimate the composition of ethane or mixed hydrate.[10,11,23,26,68,69] However, the quantitative analysis has not yet been well understood, mainly because the ambiguous assignments of some bands in the C—H stretching region and the low intensity of the C—C stretching mode of ethane in 5^{12} cages. The assignments, frequencies, FWHMs and normalized intensities of bands of ethane molecules encaged into sI deuterated hydrate and comparison with ethane bands in fluid phase are given in Table 5. Ethane hydrate was measured at 113 K and under atmospheric pressure of N_2. In this study, by referring to the assignments of ethane in fluid phase given by Helvoort et al.[67] and Domingo and Montero,[70] some ethane bands of sI C_2H_6 hydrate were assigned as the corresponding vibrational modes of ethane molecules in the LCs; other peaks were assigned as ethane in the SCs.

Raman spectrum of sI C_2H_6-D_2O hydrate in the ranges of 950–1570 and 2635–3000 cm^{-1} is illustrated in Figure 4.

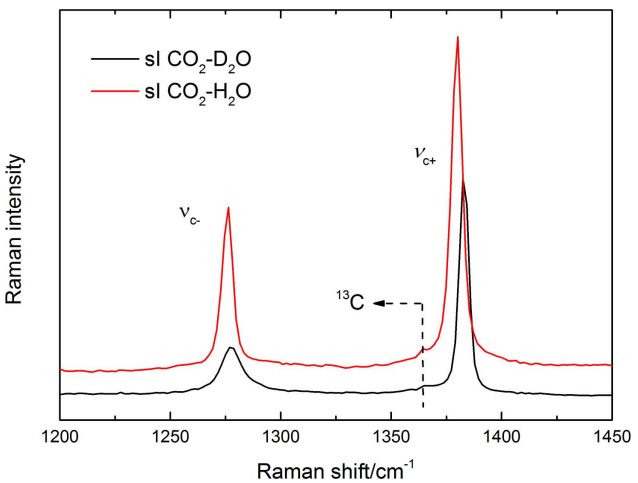

Figure 3. Representative Raman spectra of CO_2 in sI CO_2 hydrates measured at 113 K and ambient pressure.

[Color figure can be viewed in the online issue, which is available at wileyonlinelibrary.com.]

Table 4. Assignments, Gaussian/Lorentzian Ratio (y), Peak Positions and FWHMs of Raman Bands of the Deuterated and Hydrogenated sI CO_2-Hydrates Formed at 3 MPa, Measured at 113 K under Atmospheric Pressure of N_2

		sI CO_2-D_2O hydrate		sI CO_2-H_2O hydrate	
Assign.	y	ν/cm^{-1}	FWHM/cm^{-1}	ν/cm^{-1}	FWHM/cm^{-1}
ν_{c-}	0.0	1277.6 ± 0.5	11.7 ± 0.4	1275.5 ± 0.8	6.0 ± 0.3
–	0.0	1368.4 ± 1.3	15.9 ± 2.3	1366.6 ± 4.0	14.7 ± 4.0
ν_{c+}	0.51	1382.8 ± 0.5	5.3 ± 0.3	1379.4 ± 0.8	6.1 ± 0.2

Five peaks exist in the low-frequency region, see Figure 4a. The band at 999.4 cm^{-1} is related to the ^{12}C-^{12}C symmetric stretching mode (ν_3) of ethane molecules trapped in LCs, whereas on the right shoulder, a much weaker peak at approximately 1019.1 cm^{-1} is associated with the ν_3 vibration of ethane in SCs. The ν_3 band of C_2H_6 enclathrated in LCs of sI and sII hydrates is well defined with a difference of ≈8 cm^{-1};[11] this band is a very robust indicator of the structure type of gas hydrate containing ethane molecules. In the current study, it is difficult to accurately quantify the intensity ratio of ethane in the LCs to SCs using the ν_3 band because of its low-intensity resulting from the very low occupancy of ethane in SCs, see Table 5. In addition, another weak peak at 983.2 cm^{-1} originating from the ^{13}C-^{12}C stretching vibration in LCs indicates small quantity of ^{13}C is present in the studied hydrate. These peak positions obtained by the new calibration and fitting procedure are less than 3 cm^{-1} lower than our previous work.[11] The other two peaks at 1460.2 and 1546.9 cm^{-1} arising from the CH_3 deformation vibration (ν_{11})[71] and the combination of $\nu_5 + \nu_{12}$ modes of ethane in the LCs, respectively, are reported here for the first time.

In the high-frequency range, Raman spectra of sI C_2H_6-hydrate are more complicated than those of methane hydrate in the same region (see Figure 2) as a consequence of the strong multiple vibrational resonances of ethane molecules occurring among the totally symmetric C—H stretching vibration ν_1, the asymmetric CH_3—deformation overtones ($2\nu_{11}$ and $2\nu_8$), and their combinations.[70] The prominent twin bands resulting from a Fermi resonance at 2888.2 and 2942.5 cm^{-1} and an intermediate shoulder around 2924.5 cm^{-1} are assigned to the lower (ν_{e-}), upper (ν_{e+}), and intermediate (ν_{ei}) bands of the mixture of ν_1:$2\nu_{11}$:$2\nu_8$ vibrational modes of ethane in the LCs, respectively. Hirai et al.[69] and Subramanian et al.[10] gave different assignments for these three bands. One broad peak at about 2966.86 cm^{-1} is tentatively assigned as ν_{e+} modes of ethane in the SCs. This peak was seen in spectra of pure sI C_2H_6 hydrates in our earlier work, but not discussed; it is noteworthy that the corresponding peak in the sII CH_4-C_2H_6 hydrates formed from a mixture of 95 mol % CH_4 and 5 mol % C_2H_6 is not observed, likely due to the low molar fraction of ethane in the mixed hydrate.[11] A newly observed peak at approximately 2952.6 cm^{-1} is more ambiguous due to being superimposed by ν_{e+} bands. It could be related to the ν_{10} asymmetric CH-stretching mode of ethane in the LCs. Another more ambiguous peak at approximately 2907.0 cm^{-1} is associated with the ν_{e-} mode of ethane in the SCs; the experimental uncertainty here is higher than the usual ± 0.8 cm^{-1}, mainly as a result of its low intensity and overlap with other peaks. Following the same calibration procedure for sI methane hydrate, the Raman cross-section ratios of ethane in the LCs and SCs are calculated by

$$\sigma^{R}_{EL}/\sigma^{R}_{ES} = A^{R}_{EL}/3A^{R}_{ES}/\left(\theta^{D}_{EL}/\theta^{D}_{ES}\right) \quad (7)$$

Where $\theta^{D}_{EL}/\theta^{D}_{ES}$ is the cage occupancy ratio of sI ethane hydrate listed in Table 1. The determined $\sigma^{R}_{EL}/\sigma^{R}_{ES}$ ratios for the ν_{e-} and ν_{e+} bands are 0.154 ± 0.018 and 0.035 ± 0.003, respectively. These results suggest that the local environment dramatically affects the ν_{e-} and ν_{e+} vibrational modes of ethane molecules in the SCs due to the rather small size of 5^{12} cages for ethane with a resulting change of the C—H bond length. A much weaker doublet observed at 2735.2 and 2768.5 cm^{-1} can be assigned to $2\nu_6$ and $2\nu_2$ overtones even though they have a slight resonance with ν_1, respectively, as shown in Figure 4b.[70] The combination vibration $\nu_{11} + \nu_{12}$ can potentially contribute to the appearance of peak at

Table 5. Assignments, Gaussian/Lorentzian Ratio (y), Raman Shifts, FWHMs and the Normalized Peak Areas of the Observed Bands of C_2H_6 Encaged into the Deuterated sI Hydrate and Comparison with C_2H_6 in Fluid Phase

Assign.	Cage	y	ν_h/cm^{-1}	FWHM/cm^{-1}	R/%	ν_f/cm^{-1}	$\Delta\nu$/cm^{-1}
–	$5^{12}6^2$	0.0	983.2 ± 0.8	6.5 ± 2.0	0.4 ± 0.1	–	–
ν_3	$5^{12}6^2$	0.17	999.4 ± 0.0	4.0 ± 0.2	8.6 ± 1.1	992.5[a]	+6.9
–	5^{12}	0.0	1019.1 ± 1.1	15.6 ± 4.3	0.7 ± 0.2	–	+25.6
ν_{11}	$5^{12}6^2$	0.0	1460.2 ± 0.0	19.4 ± 1.4	8.3 ± 0.4	1468.4[b]	−8.2
$\nu_5 + \nu_{12}$	$5^{12}6^2$	0.54	1546.9 ± 0.1	4.2 ± 0.4	0.2 ± 0.0	–	–
$\nu_{11} + \nu_{12}$	$5^{12}6^2$	0.72	2642.5 ± 0.9	44.1 ± 10.9	1.3 ± 0.4	2658.7[b]	−16.2
$2\nu_6$	$5^{12}6^2$	0.66	2735.2 ± 0.0	4.4 ± 0.2	2.4 ± 0.1	2756.5[c]	−21.3
$2\nu_2$	$5^{12}6^2$	0.91	2768.5 ± 0.0	5.7 ± 0.1	1.1 ± 0.0	2788.7[c]	−20.2
ν_{e-}	$5^{12}6^2$	0.35	2887.2 ± 0.0	8.6 ± 0.1	25.5 ± 0.4	2896.7[c]	−9.5
–	5^{12}	1.0	2907.0 ± 3.4	31.1 ± 3.3	2.7 ± 0.3	–	+10.3
ν_{ei}	$5^{12}6^2$	0.0	2924.5 ± 0.2	7.4 ± 0.8	3.2 ± 0.4	2938.8[c]	−14.3
ν_{e+}	$5^{12}6^2$	0.35	2942.5 ± 0.0	7.0 ± 0.2	26.9 ± 0.9	2954.8[c]	−12.3
ν_{e+}	5^{12}	1	2966.9 ± 0.0	12.3 ± 0.6	12.2 ± 0.9	–	+12.1
ν_{10}	$5^{12}6^2$	0.0	2952.6 ± 0.3	20 ± 1.4	6.6 ± 0.7	2968.7[c]	−16.1

ν_h and ν_f indicate Raman frequencies of ethane in hydrate lattices and fluid phase, respectively. R is percentage of peak area.
[a,b] and [c] represent the values given by Helvoort et al.[67], Fernandez and Montero[71], and Domingo and Montero[70], respectively. $\Delta\nu$ is the difference between ν_h and ν_f.

Table 6. Results of the Experimentally Determined Ratios of F-factors of CO_2 and C_2H_6 with Respect to CH_4 in D_2O or H_2O Hydrate Lattices and Comparison with the Established Values in Fluid Phase

	C_2H_6			CO_2		
F_E/F_M	sI C_2H_6-D_2O	Fluid	F_C/F_M	sI CO_2-D_2O	sI CO_2-H_2O	Fluid
F_{999}/F_{2901}	0.21 ± 0.03	0.21[a]	F_{1278}/F_{2913}	0.13 ± 0.01	0.13 ± 0.01	0.13[b]
F_{2887}/F_{2901}	0.63 ± 0.03	–	F_{1383}/F_{2913}	0.24 ± 0.02	0.26 ± 0.02	0.2[b], 0.34[d]
F_{2907}/F_{2913}	4.14 ± 0.55	–	F_{CT}/F_{2913}	0.37 ± 0.03	0.39 ± 0.04	0.77[e]
F_{2942}/F_{2901}	0.67 ± 0.04	1.76[b]				
F_{2967}/F_{2913}	18.81 ± 1.68	–				
F_{ET}/F_{2901}	1.38 ± 0.07	2.2[c]				

[a]The value quoted from Schrötter and Klöckner[51] was converted using the Eq. 1 in the reference[48];
[b]ratios of F-factor were calculated by the given cross sections[48];
[c]and [e] are estimations from the graph in Subramanian et al.[10] and Sum et al.[23], respectively; [d]data are taken from the Seitz et al.[37]; F_{ET} and F_{CT} represent the Raman quantification factors were calculated by the sum area of the ν_{e-}, ν_{ei} and ν_{e+} bands of C_2H_6 in the LCs and Fermi diad of CO_2, respectively.

2642.5 cm^{-1}. These three peaks are reported for the first time for ethane in the hydrate phase.

The difference between the band positions of C_2H_6 in sI ethane hydrate (ν_h) and in fluid phase (ν_f), $\Delta\nu = \nu_f - \nu_h$, are also listed in Table 5. It can be seen that $\Delta\nu$'s for ethane in the SCs are all positive, and those in the LCs are negative, except for the C—C vibrational band. Using the semiempirical "loose cage-tight cage" model, Subramanian and Sloan[15] also elucidated that, compared with the corresponding band positions of C_2H_6 in vapor phase, the ν_3 band positions of ethane in LCs and SCs of sI ethane hydrate have a smaller (6.5 cm^{-1}) and larger (25.6 cm^{-1}) positive Raman shift, respectively, whereas the ν_{e-} and ν_{e+} bands of ethane in LCs show a negative shift. Our results are consistent with their report.

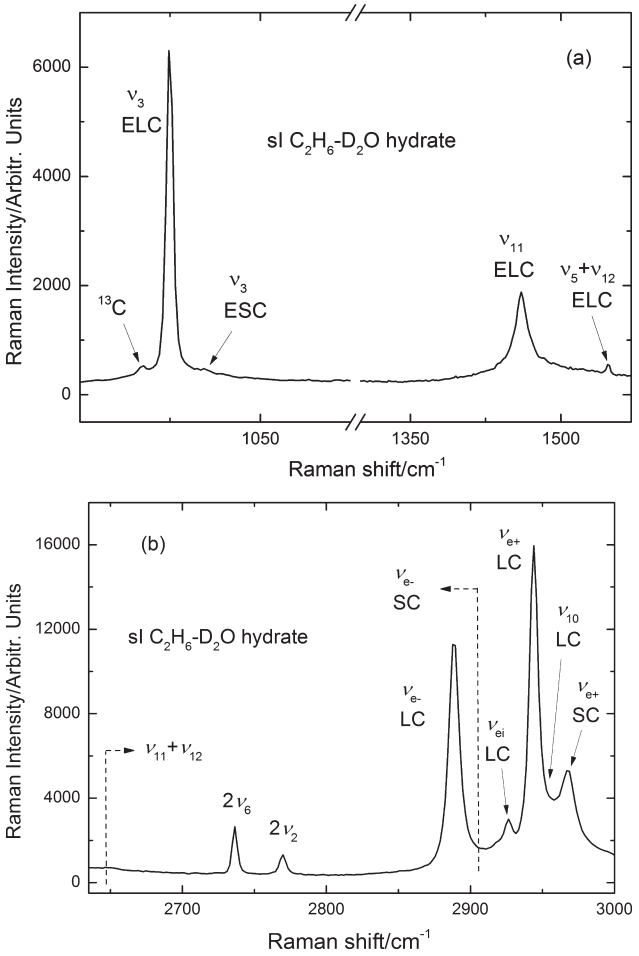

Figure 4. Typical Raman spectra of sI C_2H_6-D_2O hydrate in the range (a) 950–1570 cm^{-1}, and (b) 2635–3000 cm^{-1}.

Raman spectra of the hydrate framework

Raman bands of the deuterated framework of sI gas hydrates can be separated into two main regions: the D_2O translational (100–400 cm^{-1}) and the O—D stretching (2100–2830 cm^{-1}) regions, while those of the hydrogenated host can be classified into H_2O translational and the O—H stretching (2830–3600 cm^{-1}) vibrations. In this work, only the O—D and O—H stretching bands of host molecules were considered to calibrate the relative F-factors of different guest molecules. Figure 5 shows Raman spectra of pure sI deuterated hydrates of CO_2, C_2H_6 and CH_4 in the O—D stretching region and sI hydrogenated hydrates of CO_2, and CH_4 in the O—H stretching region. It can be seen that shapes of these bands measured at 113 K under ambient pressure of N_2 are quite similar. Schicks et al.[59] found that Raman peaks in the O—H stretching range are similar between the pure H_2O ice I_h and sI CH_4-hydrate, whereas they are clearly different for sII CH_4-hydrate. Uras-Aytemiz and coworkers[72] analyzed aerosols of gas hydrates nanoparticles by FTIR spectroscopy and showed

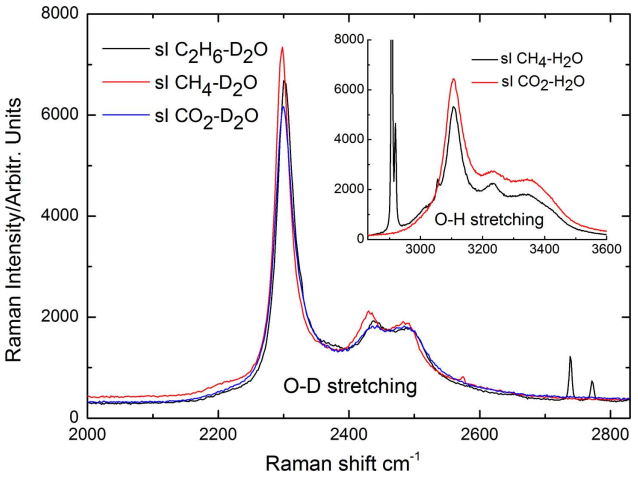

Figure 5. Typical Raman spectra of the O-D stretching vibrational bands of pure deuterated sI CO_2-, C_2H_6- and CH_4-hydrates and the O-H stretching vibrational bands of pure hydrogenated sI CO_2- and CH_4-hydrates (inset).

[Color figure can be viewed in the online issue, which is available at wileyonlinelibrary.com.]

the good agreement of spectra of the D_2O or H_2O frameworks of different deuterated or hydrogenated gas hydrates containing CO_2, CH_4, C_2H_2, etc. The similarity of these spectra suggests that the influence of guest–host interactions onto Raman O—D and O—H stretching vibrations is small. Consequently, the assumption is made in the following that the O—D and O—H stretching Raman signals of host lattices are independent of guest molecules investigated here, which makes them suitable as an internal calibrant for the amount of hydrate in the beam if no ice I_h is present.

Raman quantification factor

In this study, the relative Raman quantification factors of gas hydrates are given in two ways: guest to guest and guest to host framework. Ratios of F-factors of the specific vibrational modes of the trapped CO_2 and C_2H_6 molecules to CH_4 in sI hydrates, F_C/F_M and F_E/F_M, were determined by comparing the spectra of CH_4-hydrate with two consecutive measurements of CO_2- and C_2H_6-hydrates. Peak areas of this set of different spectra are comparable following the experimental procedure discussed above section. On the other hand, the relative F-factor of guest to D_2O or H_2O host, F/F^H, was directly calculated by the corresponding intensities of peaks within the same spectrum. Pure sI CH_4-hydrates formed at 6 MPa, CO_2-hydrates synthesized at 3.5 MPa and C_2H_6-D_2O hydrate synthesized at 3.8 MPa were used for this purpose (see Table 1).

According to Eq. 1, the integrated area of O—D stretching bands of D_2O hydrate is proportional to the number of D_2O molecules in the sampled volume; the same argument also holds for H_2O hydrate. Under the assumption that Raman spectra of host molecules in pure sI CO_2-, CH_4- and C_2H_6-hydrates are independent of the guest species, two scaling factors are introduced

$$C_{CM} = A_C^H / A_M^H \tag{8}$$

$$C_{EM} = A_E^H / A_M^H \tag{9}$$

where C_{CM} refers to the scaling factor of CO_2 to CH_4, C_{EM} is the scaling factor between C_2H_6 and CH_4, A'_C, A'_M and A'_E represent the integration area of the O—D stretching modes of host molecules in 2100–2830 cm^{-1} or those of O—H bands in 2830–3600 cm^{-1}, respectively. By comparing these two factors, the same amount of host molecules as in sI CH_4 hydrate as in two almost concomitant measurements of sI CO_2- and C_2H_6-hydrates are derived. As a result, F_C/F_M and F_E/F_M can be obtained from pure CO_2-, CH_4- and C_2H_6-hydrates with the cage fillings established from synchrotron powder diffraction (see Table 1).

As demonstrated earlier, Raman spectra of CH_4 and C_2H_6 molecules trapped into the LCs and SCs of sI hydrate cavities are both well-defined, while CO_2 cannot be resolved in this study. The relative F-factors of the bands resulting from C_2H_6 in the LCs or SCs to the v_1 bands of CH_4 in the LCs or SCs are given by the following expressions

$$F_{EL}/F_{ML} = \frac{(A_{EL}/A_{ML})/(\theta_{EL}/\theta_{ML})}{C_{EM}} \tag{10}$$

$$F_{ES}/F_{MS} = (A_{ES}/A_{MS})/(\theta_{ES}/\theta_{MS})/C_{EM} \tag{11}$$

Considering that Raman bands of the encaged CO_2 molecules in the LCs and SCs cannot be resolved, the nontrivial assumption is made that the Raman cross sections of CO_2 in the LCs and SCs are identical. F_C/F_M can be obtained by

$$F_C/F_{MS} = A_C \Big/ \left(\frac{A_{ML} \times \theta_{CL}}{\theta_{ML} \times \sigma_{ML}/\sigma_{MS}} + \frac{A_{MS} \times \theta_{CS}}{\theta_{MS}} \right) / C_{CM} \tag{12}$$

where σ_{ML}/σ_{MS} is 0.977 for sI CH_4-H_2O, and 0.974 for sI CH_4-D_2O hydrate, see Table 3.

Table 7. Results of the Experimentally Determined Ratios of F-factors of Guests to Host Molecules in the Deuterated or Hydrogenated sI CH_4-, CO_2- and C_2H_6-Hydrates

		Framework	
Hydrate	F/F^H	D_2O	H_2O
sI CH_4	F_{2901}/F_M^H	1.12 ± 0.04	0.95 ± 0.06
	F_{2913}/F_M^H	1.13 ± 0.04	1.03 ± 0.07
sI CO_2	F_{1278}/F_C^H	0.15 ± 0.01	0.12 ± 0.01
	F_{1383}/F_C^H	0.27 ± 0.03	0.25 ± 0.02
	F_{CT}/F_C^H	0.42 ± 0.04	0.38 ± 0.02
sI C_2H_6	F_{2887}/F_E^H	0.71 ± 0.03	–
	F_{2907}/F_E^H	4.66 ± 0.57	–
	F_{2942}/F_E^H	0.75 ± 0.04	–
	F_{2967}/F_E^H	21.17 ± 1.67	–

F^H refers to the Raman quantification factor of the O—D or O—H stretching-vibrational bands of the host molecules.

Results of F_C/F_M and F_E/F_M are listed in Table 6. It can be seen that Raman quantification factors of v_{e-}, v_{ei} and v_{e+} bands of C_2H_6 encaged into sI D_2O hydrate are apparently different. Domingo and Montero[70] also reported the different cross sections of these three bands of C_2H_6 in gas phase. Intensities of peaks centered at 2887.2 and 2942.5 cm^{-1} or the sum of 2887.2, 2952.6 and 2942.5 cm^{-1} are suggested reflecting the molar fraction of C_2H_6 in the LCs, because the uncertainty of their F-factors based on all the measurements are within ±6%, see Table 6. Area ratios of A_{2967}/A_{2913} and A_{2907}/A_{2913} can be used to determine composition of the SCs. The relative F-factor of CO_2 to CH_4, F_C/F_M, derived from H_2O and D_2O host frameworks are identical for v_{c-} band, and slightly different for v_{c+} band. This may mean that ratios of F-factors are assumed to be independent of the isotopic composition of the hydrate framework. Consequently, the empirical F_E/F_M obtained by pure sI deuterated C_2H_6- and CH_4-hydrates can also be applied for the sI hydrogenated gas hydrates in good approximation.

It is interesting to compare these results in the hydrate phase with the published F-factors of guests in the fluid phase. As shown in Table 6, the relative F-factors relating the v_{c-} band of CO_2 in H_2O and D_2O hydrates to the stretching-vibrational peaks of CH_4 in the LCs and SCs of H_2O and D_2O hydrates, F_{1278}/F_{2913}, are identical to the corresponding ratio of CO_2 to CH_4 in the vapor phase, whereas ratio of F-factors of the v_{c+} bands to CH_4 in the LCs and SCs are up to 30% higher than values published by Burke[48] and 30% lower than given by Seitz.[37] The estimated F_{CT}/F_M ($_{CT}$ means the sum of the Fermi dyad) from the graph given by Sum et al.[23] is almost two times higher than our result. The relative F-factor relating the C—C stretching band of C_2H_6 to CH_4 in LCs agrees with the result of C_2H_6 and CH_4 in gas phase,[51] even though the uncertainty of our result is larger than 10%. However, a considerable discrepancy occurs for the C—H stretching region of C_2H_6. Comparing the sum of peak areas of v_{e-}, v_{ei} and v_{e+} of C_2H_6 (A_{ET}) with v_1 band of CH_4 in gas phase, Subramanian et al.[10] reported F_{ET}/F_M to be around 2.2 (estimation from the given

Table 8. The Cage Occupancies of Guests in the LCs and SCs, and Total Cage Occupancies of Guests Trapped into the Deuterated sI CO_2-C_2H_6-CH_4 Hydrate Calculated with the Empirical F-factors

Cage	θ_C/%	θ_M/%	θ_E/%
$5^{12}6^2$	–	35.9 ± 1.3	24.1 ± 1.3
5^{12}	–	69.3 ± 2.5	1.0 ± 0.0
Total	26.3 ± 1.7	44.3 ± 1.6	18.3 ± 1.0

graph). It is approximately 60% higher than our result for sI gas hydrates. The ratio of Raman scattering cross sections of ν_{e+} band of C_2H_6 to CH_4 in gas phase given by Burke[48] is approximately 2.6 times higher than our determination. It can be concluded that the previous assumption that Raman scattering cross section of species keeps constant when free molecules in fluid phase are encaged into the hydrate cavities are an oversimplification.[10,23]

Using the ratios of Raman quantification factors between guests, the relative abundance of guests in different cages and bulk composition of guests in the mixed gas hydrates containing CH_4, CO_2 and C_2H_6 can be determined. On the other hand, the absolute cage occupancies and bulk composition of gas hydrate can be derived from the relative F-factor of guest to host framework. Comparing peak area of the O—D or O—H stretching-vibrational bands of D_2O or H_2O host framework with the splitting bands of CH_4 or C_2H_6 molecules in different cages of pure sI CH_4- or C_2H_6-hydrate, the relative F-factors of CH_4 or C_2H_6 in the LCs and SCs to host molecules are obtained by

$$F_L/F^H = A_L \times 46/\left(A^H \times 6 \times \theta_L\right) \quad (13)$$

$$F_S/F^H = A_S \times 46/\left(A^H \times 2 \times \theta_S\right) \quad (14)$$

respectively, where 46, 6 and 2 are the number of H_2O or D_2O molecules, the large and small cages per unit cell of sI gas hydrate. For pure sI CO_2-hydrate F_C/F_C^H, is calculated by

$$F_C/F_C^H = A_C/A_C^H \times 46/(6 \times \theta_{CL} + 2 \times \theta_{CS}) \quad (15)$$

The determined results are shown in Table 7. It can be seen that for pure sI CH_4- and CO_2- hydrates, the relative F-factors in D_2O framework are 8–25% higher than those in H_2O framework. The difference between the cross sections of the same guest molecules in D_2O hydrates cavities and those in H_2O cavities was experimentally established for the first time.

Our calibration strategy provides a workable approach which appears to be more realistic for gas hydrates than the previous methodology, and is expected to deliver more accurate results. To accurately determine the compositional information of gas hydrates, a calibration protocol for the relative Raman quantification factor as proposed in this study should be considered, instead of applying the available cross sections or ratios of F-factor of guests in fluid phase. In addition, the results are also helpful for a better understanding of the interactions of guests and host framework. It should be noted that the cross sections of guests may vary with cage occupancy and guest composition, both possibly mediated by the resulting slight change in the host framework geometry. In this study, the relative Raman quantification factor are calibrated by one set of gas hydrates with known cage occupancies; further work is needed to study the dependency of the relative Raman scattering cross sections for gas hydrates with different cage fillings.

Application

The relative Raman quantification factors obtained in this study can be used to determine the compositional information of the synthetic and natural sI gas hydrates containing CH_4, CO_2 and/or C_2H_6 in terms of the cage occupancies, the guest composition and hydration number, etc. In particular, for *in situ* Raman investigation on CH_4-hydrate replaced by CO_2 molecules, F_C/F_M and F_C/F_C^H can be applied to infer the local replacement ratio. As mentioned previously, the Raman scattering cross section ratio of CH_4 in the LCs and SCs of sI CH_4 hydrate is close to 1, while the LC/SC ratio of the ν_{e+} band of C_2H_6 in sI hydrate is down to 0.035. This implies that the difference between the cage size and guest molecule size sometimes plays an important role in determining the Raman quantification factor of guest. However, considering the variation of cage size between sI and sII hydrates, the difference for the cross section of CH_4 in a sII structure is not expected to be substantially bigger than the 2–3% difference between methane in the small and large cage in a sI structure. For larger molecules, CO_2 and C_2H_6, the cross section difference may be larger between sI and sII hydrates. Thus, for the price of an additional uncertainty of the F-factor ratio of 5–10%, our results can also be applied to sII CO_2 and C_2H_6 hydrates. Please note, that considering the very high sensitivity of the ethane Raman cross section in the small cage, intercomparisons of the ethane cage occupancies in sII hydrates should be restricted to the large cages.

To apply the empirical Raman quantification factors derived from the comparison of the Raman spectra of pure sI gas hydrates to the mixed system, three assumptions are made:

1. The interactions between guests and the host framework, and among the weakly polar guests located in neighboring cages, such as CH_4, CO_2 or C_2H_6, are small enough to be negligible.
2. The relative Raman quantification factors are independent of the cage occupancies and composition of guests as mediated by the host framework.
3. No ice exists in the system.

While assumption 1 is usually considered acceptable, assumption 2 is not trivial as the water framework and the resulting cage geometry will be affected by variations of cage occupancies and guest type. According to our neutron or X-ray powder diffraction results, the content of pure ice in the clathrate material produced in our laboratory is quite small going up to a few wt %.[73] Clearly, it is important to determine the concentration of pure ice in the specific gas hydrates under investigation (e.g., by diffraction) before empirical F-factors are applied.

Figure 6 shows one Raman spectrum of sI deuterated hydrate containing CH_4-CO_2-C_2H_6 mixture with unknown composition. Using the determined F-factors between guest and host molecules, the absolute cage occupancies in $5^{12}6^2$ (θ_L) and 5^{12} cages (θ_S), and the total cage occupancies of CH_4 or C_2H_6 (θ) are determined by the following expressions

$$\theta_L = A_L \times 46 \,/\left(A^H \times 6\right)/\left(F_L/F^H\right) \quad (16)$$

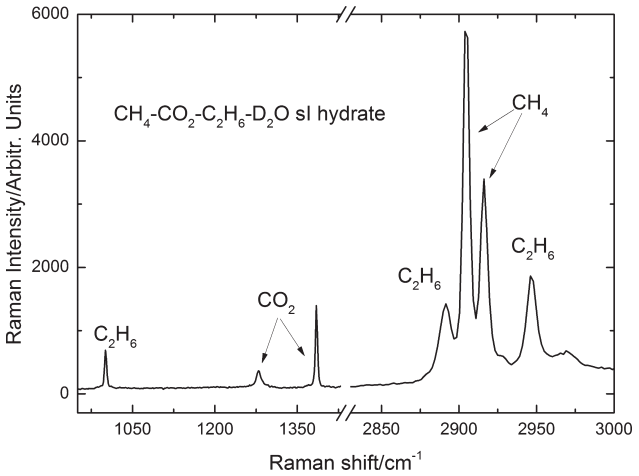

Figure 6. Raman spectra of the deuterated sI CH_4-CO_2-C_2H_6-hydrate measured at ambient pressure and 113 K.

$$\theta_S = A_S \times 46 \,/\left(A^H \times 2\right)/\left(F_S/F^H\right) \quad (17)$$

$$\theta = (\theta_L \times 6 + \theta_S \times 2)/8 \quad (18)$$

while the total cage occupancy of CO_2 (θ_C) is calculated by

$$\theta_C = A_C \times 46 \,/\left(A_C^H \times F_C/F_C^H\right)/8 \quad (19)$$

The relative F-factors presented in this work (Table 7), F_{2901}/F_M^H, F_{2913}/F_M^H, F_{2942}/F_E^H, F_{2967}/F_E^H, F_{1278}/F_M^H and their corresponding intensities of Raman bands were used to determine the cage occupancies of sI deuterated CH_4-CO_2-C_2H_6-hydrate, see Table 8. The uncertainty of the cage occupancies arises from the uncertainty of the relative F-factors. Not unexpected, but established here in a quantitative manner, methane occupies both the small and large cages, whereas ethane prefers to reside in the LCs. The total cage occupancy of CH_4, C_2H_6 and CO_2 is 88.5 ± 4.3 in percentage, and the bulk guest composition is around 50.0 ± 1.3%mol CH_4, 20.6 ± 0.5%mol C_2H_6 and 29.4 ± 1.8%mol CO_2. Therefore, the calculated hydration number is 6.50 ± 0.25 using Eq. 4. The estimated uncertainty in the hydration number is less than 4%, which permits to establish the composition of the mixed hydrates with useful precision.

Conclusion

Raman spectroscopy is a standard method for the qualitative and semiquantitative analyses of gas hydrates in chemical engineering applications. With some additional calibration effort, it is also a promising useful tool for providing the quantitative information of pure and mixed gas hydrates as demonstrated here for the calibration of Raman quantification factor of guests in the deuterated and hydrogenated sI CO_2-, CH_4- and C_2H_6-hydrates on the basis of the guest molecules' specific Raman bands.

The Raman scattering cross sections of CH_4 molecules enclathrated into 5^{12} and $5^{12}6^2$ cages are found to be different by directly comparing the analysis of Raman spectroscopy with the absolute cage fillings established by synchrotron X-ray powder diffraction; the difference is small but significant. This slight difference should be taken into consideration for the future determination of the hydration number of methane hydrate. To proceed in the case of ethane hydrate, we have tentatively assigned Raman bands as ethane molecules trapped into the LCs and SCs by a comparison with the corresponding lines of ethane in fluid phase.

The relative Raman quantification factors of guest to guest and guest to host molecules, were obtained by analyzing the specific peak areas of pure sI CO_2-, CH_4- and C_2H_6-hydrates with known cage occupancies obtained from synchrotron powder diffraction. Our results are considered to be more accurate than the available values of guests calibrated in fluid phase. Under several assumptions, the empirical F-factors can be used for the quantitative analysis of the mixed gas hydrates containing CO_2-, CH_4- and C_2H_6.

Acknowledgment

We thank Dr. Andrzej Falenty (Göttingen), Dr. M. Mangir Murshed (Göttingen and Bremen), Dr. Burkhard C. Schmidt (Göttingen) and Christiane D. Hartmann (Göttingen) for experimental help and useful discussions. This research was supported by the German Ministry of Education and Research (BMBF) in the framework of the special program GEOTECHNOLOGIEN and within the SUGAR-II research initiative by the grant 03G0819B (TP B2–3).

Literature Cited

1. Sloan ED, Koh CA. Clatherate Hydrates of Natural Gases. 3rd ed. Boca Raton, FL: CRC Press; 2008.
2. Koh CA. Towards a fundamental understanding of natural gas hydrates. *Chem Soc Rev*. 2002;31:157–167.
3. Chou IM, Sharma A, Burruss RC, Shu JF, Mao HK, Hemley RJ, Goncharov AF, Stern LA, Kirby SH. Transformations in methane hydrates. *Proc Nat Acad Sci USA*. 2000;97:13484–13487.
4. Kurnosov AV, Ogienko AG, Goryainov SV, Larionov EG, Manakov AY, Lihacheva AY, Aladko EY, Zhurko FV, Voronin VI, Berger IF, Ancharov AI. Phase diagram and high-pressure boundary of hydrate formation in the ethane-water system. *J Phys Chem B*. 2006;110: 21788–21792.
5. Loveday JS, Nelmes RJ. High-pressure gas hydrates. *Phys Chem Chem Phys*. 2008;10:937–950.
6. Hirai H, Komatsu K, Honda M, Kawamura T, Yamamoto Y, Yagi T. Phase changes of CO_2 hydrate under high pressure and low temperature. *J Chem Phys*. 2010;133:124511.
7. Staykova DK, Kuhs WF, Salamatin AN, Hansen T. Formation of porous gas hydrates from ice powders: Diffraction experiments and multistage model. *J Phys Chem B*. 2003;107:10299–10311.
8. Schicks JM, Ripmeester JA. The coexistence of two different methane hydrate phases under moderate pressure and temperature conditions: Kinetic versus thermodynamic products. *Angew Chem Int Ed*. 2004;43:3310–3313.
9. Choukroun M, Morizet Y, Grasset O. Raman study of methane clathrate hydrates under pressure: new evidence for the metastability of structure II. *J Raman Spectrosc*. 2007;38:440–451.
10. Subramanian S, Kini RA, Dec SF, Sloan ED. Evidence of structure II hydrate formation from methane plus ethane mixtures. *Chem Eng Sci*. 2000;55:1981–1999.
11. Murshed MM, Kuhs WF. Kinetic studies of methane-ethane mixed gas hydrates by neutron diffraction and Raman spectroscopy. *J Phys Chem B*. 2009;113:5172–5180.
12. Uchida T, Kida M, Nagao J. Dissociation termination of methane-ethane hydrates in temperature-ramping tests at atmospheric pressure below the melting point of ice. *Chemphyschem*. 2011;12:1652–1656.
13. Schicks JM, Naumann R, Erzinger J, Hester KC, Koh CA, Sloan ED, Jr. Phase transitions in mixed gas hydrates: Experimental observations versus calculated data. *J Phys Chem B*. 2006;110:11468–11474.
14. Lee H, Seo Y, Seo YT, Moudrakovski IL, Ripmeester JA. Recovering methane from solid methane hydrate with carbon dioxide. *Angew Chem. Int Ed*. 2003;42:5048–5051.
15. Subramanian S, Sloan ED. Trends in vibrational frequencies of guests trapped in clathrate hydrate cages. *J Phys Chem B*. 2002;106: 4348–4355.

16. Milkov AV. Global estimates of hydrate-bound gas in marine sediments: how much is really out there? *Earth Sci Rev*. 2004;66:183–197.
17. Klauda JB, Sandler SI. Global distribution of methane hydrate in ocean sediment. *Energy Fuels*. 2005;19:459–470.
18. Boswell R, Collett TS. Current perspectives on gas hydrate resources. *Energy Environ Sci*. 2011;4:1206–1215.
19. Maslin M, Owen M, Betts R, Day S, Dunkley Jones T, Ridgwell A. Gas hydrates: past and future geohazard? *Phil Trans R Soc A*. 2010;368:2369–2393.
20. Ohgaki K, Takano K, Sangawa H, Matsubara T, Nakano S. Methane exploitation by carbon dioxide from gas hydrates - Phase equilibria for CO_2-CH_4 mixed hydrate system. *J Chem Eng Jpn*. 1996;29:478–483.
21. Yoon JH, Kawamura T, Yamamoto Y, Komai T. Transformation of methane hydrate to carbon dioxide hydrate: In situ Raman spectroscopic observations. *J Phys Chem A*. 2004;108:5057–5059.
22. Ota M, Morohashi K, Abe Y, Watanabe M, Smith RL, Inomata H. Replacement of CH_4 in the hydrate by use of liquid CO_2. *Energy Convers Manage*. 2005;46:1680–1691.
23. Sum AK, Burruss RC, Sloan ED. Measurement of clathrate hydrates via Raman spectroscopy. *J Phys Chem B*. 1997;101:7371–7377.
24. Uchida T, Hirano T, Ebinuma T, Narita H, Gohara K, Mae S, Matsumoto R. Raman spectroscopic determination of hydration number of methane hydrates. *AIChE J*. 1999;45:2641–2645.
25. Tulk CA, Ripmeester JA, Klug DD. The application of Raman spectroscopy to the study of gas hydrates. In: Holder GDBPR, ed. Gas Hydrates: Challenges for the Future. Vol 912. New York Academy of Sciences; 2000:859–872.
26. Uchida T, Takeya S, Kamata Y, Ikeda IY, Nagao J, Ebinuma T, Narita H, Zatsepina O, Buffett BA. Spectroscopic observations and thermodynamic calculations on clathrate hydrates of mixed gas containing methane and ethane: determination of structure, composition and cage occupancy. *J Phys Chem B*. 2002;106:12426–12431.
27. Chazallon B, Focsa C, Charlou JL, Bourry C, Donval JP. A comparative Raman spectroscopic study of natural gas hydrates collected at different geological sites. *Chem. Geol*. 2007;244:175–185.
28. Lu HL, Ripmeester JA. A laboratory protocol for the analysis of natural gas. Paper presented at: Proceedings of the 6th International Conference on Gas Hydrates; July 6–10, 2008; Vancouver, BC, Canada.
29. Ripmeester JA, Ratcliffe CI. Low-temperature cross-polarization/magic angle spinning ^{13}C NMR of solid methane hydrates: structure, cage occupancy, and hydration number. *J Phys Chem*. 1988;92:337–339.
30. Rovetto LJ, Bowler KE, Stadterman LL, Dec SF, Koh CA, Sloan ED. Dissociation studies of CH_4-C_2H_6 and CH_4-CO_2 binary gas hydrates. *Fluid Phase Equilib*. 2007;261:407–413.
31. Moudrakovski I, Lu HL, Ripmeester JA. Experimental solid state NMR of gas hydrates: problems and solutions. Paper presented at: Proceedings of the 6th International Conference on Gas Hydrates; July 6–10, 2008; Vancouver, BC, Canada.
32. Susilo R, Ripmeester JA, Englezos P. Characterization of gas hydrates with PXRD, DSC, NMR, and Raman spectroscopy. *Chem Eng Sci*. 2007;62:3930–3939.
33. Kumar R, Linga P, Moudrakovski I, Ripmeester JA, Englezos P. Structure and kinetics of gas hydrates from methane/ethane/propane mixtures relevant to the design of natural gas hydrate storage and transport facilities. *AIChE J*. 2008;54:2132–2144.
34. Murshed MM, Schmidt BC, Kuhs WF. Kinetics of methane-ethane gas replacement in clathrate-hydrates studied by time-resolved neutron diffraction and Raman spectroscopy. *J Phys Chem A*. 2010;114:247–255.
35. Kuhs WF, Hansen TC. Time-resolved neutron diffraction studies with emphasis on water ices and gas hydrates. In: Wenk HR, ed. Neutron Scattering in Earth Sciences. Chantilly, VA: Mineralogical Society of America; 2006;63:171–204.
36. Anthonsen JW. Raman-spectra of some halogen gas hydrates. *Acta Chem Scand Ser A*. 1975;29:175–178.
37. Seitz JC, Pasteris JD, Wopenka B. Characterization of CO_2-CH_4-H_2O fluid inclusions by microthermometry and laser Raman microprobe spectroscopy: Inferences for clathrate and fluid equilibria. *Geochim Cosmochim Acta*. 1987;51:1651–1664.
38. Nakahara J, Shigesato Y, Higashi A, Hondoh T, Langway CC. Raman-spectra of natural clathrates in deep ice cores. *Philos Mag B*. 1988;57:421–430.
39. Uchida T, Takagi A, Kawabata J, Mae S, Hondoh T. Raman-spectroscopic analyses on the growth-process of CO_2 hydrates. *Energy Convers Manage*. 1995;36:547–550.
40. Pimentel GC, Charles SW. Infrared spectral perturbations in matrix experiments. *Pure Appl Chem*. 1963;7:111–123.
41. Uchida T, Okabe R, Mae S, Ebinuma T, Narita H. In situ observations of methane hydrate formation mechanisms by Raman spectroscopy. In: Holder GD, Bishnoi PR, eds. Gas Hydrates: Challenges for the Future. Vol 912: New York Academy of Sciences; 2000:593–601.
42. Ripmeester JA, Ratcliffe CI. The diverse nature of dodecahedral cages in clathrate hydrates as revealed by ^{129}Xe and ^{13}C NMR spectroscopy: CO_2 as a small-cage guest. *Energy Fuels*. 1998;12:197–200.
43. Takeya S, Udachin KA, Moudrakovski IL, Susilo R, Ripmeester JA. Direct space methods for powder X-ray diffraction for guest-host materials: Applications to cage occupancies and guest distributions in clathrate hydrates. *J Am Chem Soc*. 2010;132:524–531.
44. Wilson LD, Tulk CA, Ripmeester JA. Instrumental techniques for the investigation of methane hydrate: cross-callibrating NMR and Raman spectroscopic data. Paper presented at: Proceedings of the 4th International Conference on Gas Hydrates; May 19–23, 2002; Yokohama, Japan.
45. Uchida T, Takeya S, Wilson LD, Tulk CA, Ripmeester JA, Nagao J, Ebinuma T, Narita H. Measurements of physical properties of gas hydrates and in situ observations of formation and decomposition processes via Raman spectroscopy and X-ray diffraction. *Can J Phys*. 2003;81:351–357.
46. Wopenka B, Pasteris JD. Raman intensities and detection limits of geochemically relevant gas-mixtures for a laser Raman microprobe. *Anal Chem*. 1987;59:2165–2170.
47. Dubessy J, Poty B, Ramboz C. Advances in C—O—H—N—S fluid geochemistry based on micro-Raman spectrometric analysis of fluid inclusions. *Euro J Mineral*. 1989;1:517–534.
48. Burke EAJ. Raman microspectrometry of fluid inclusions. *Lithos*. 2001;55:139–158.
49. Seitz JC, Pasteris JD, Chou IM. Raman spectroscopic characterization of gas mixtures.2. Quantitative composition and pressure determination of the CO_2-CH_4 system. *Am J Sci*. 1996;296:577–600.
50. Chou IM, Pasteris JD, Seitz JC. High-density volatiles in the system C—O—H—N for the calibration of a laser Raman microprobe. *Geochim Cosmochim Acta*. 1990;54:535–543.
51. Schrötter HW, Klöckner HW. Raman scattering cross sections in gases and liquids. In: Webber A, ed. Raman Spectroscopy of Gases and Liquids. Berlin, Germany: Springer-Verlag; 1979:123–166.
52. Chazallon B, Champagnon B, Panczer G, Pauer F, Klapproth A, Kuhs WF. Micro-Raman analysis of synthetic air clathrates. *Euro J Mineral*. 1998;10:1125–1134.
53. Hartmann CD, SHemes S, Falenty A, Kuhs WF. The structure and cage filling of gas hydrates as established by synchrotron powder diffraction data. Paper presented at: Proceedings of the 7th International Conference on Gas Hydrates; July 17–21, 2011; Edinburgh, Scotland, UK.
54. Genov G, Kuhs WF, Staykova DK, Goreshnik E, Salamatin AN. Experimental studies on the formation of porous gas hydrates. *Am Mineral*. 2004;89:1228–1239.
55. Kuhs WF, Staykova DK, Salamatin AN. Formation of methane hydrate from polydisperse ice powders. *J Phys Chem B*. 2006;110:13283–13295.
56. Massiot D, Fayon F, Capron M, King I, Le Calve S, Alonso B, Durand JO, Bujoli B, Gan ZH, Hoatson G. Modelling one- and two-dimensional solid-state NMR spectra. *Magn Reson Chem*. 2002;40:70–76.
57. Lu WJ, Chou IM, Burruss RC, Song YC. A unified equation for calculating methane vapor pressures in the CH_4-H_2O system with measured Raman shifts. *Geochim Cosmochim Acta*. 2007;71:3969–3978.
58. Ohno H, Kida M, Sakurai T, Iizuka Y, Hondoh T, Narita H, Nagao J. Symmetric stretching vibration of ch_4 in clathrate hydrate structures. *Chemphyschem*. 2010;11:3070–3073.
59. Schicks JM, Erzinger J, Ziemann MA. Raman spectra of gas hydrates - differences and analogies to ice Ih and (gas saturated) water. *Spectrochim Acta Part A*. 2005;61:2399–2403.
60. Hester KC, Dunk RM, White SN, Brewer PG, Peltzer ET, Sloan ED. Gas hydrate measurements at hydrate ridge using Raman spectroscopy. *Geochim Cosmochim Acta*. 2007;71:2947–2959.

61. Hiratsuka M, Ohmura R, Sum AK, Yasuoka K. Molecular vibrations of methane molecules in the structure I clathrate hydrate from ab initio molecular dynamics simulation. *J Chem Phys*. 2012;136:144306.
62. Chazallon B, Itoh H, Koza M, Kuhs WF, Schober H. Anharmonicity and guest-host coupling in clathrate hydrates. *Phys Chem Chem Phys*. 2002;4:4809–4816.
63. Charlou JL, Donval JP, Fouquet Y, Ondreas H, Knoery J, Cochonat P, Levache D, Poirier Y, Jean-Baptiste P, Fourre E, Chazallon B, Party ZLS. Physical and chemical characterization of gas hydrates and associated methane plumes in the Congo-Angola Basin. *Chem Geol*. 2004;205:405–425.
64. Ikeda T, Mae S, Uchida T. Effect of guest-host interaction on Raman spectrum of a CO2 clathrate hydrate single crystal. *J Chem Phys*. 1998;108:1352–1359.
65. Kuhs WF, Chazallon B, Klapproth A, Pauer F. Filling isotherms in clathrate hydrates. *Rev High Pressure Sci Technol*. 1998;7:1147–1149.
66. Morizet Y, Paris M, Gaillard F, Scaillet B. Raman quantification factor calibration for CO—CO_2 gas mixture in synthetic fluid inclusions: Application to oxygen fugacity calculation in magmatic systems. *Chem Geol*. 2009;264:58–70.
67. Helvoort KV, Knippers W, Fantoni R, Stolte S. The Raman-spectrum of ethane from 600 to 6500 cm^{-1} stokes shifts. *Chem Phys*. 1987;111:445–465.
68. Morita K, Nakano S, Ohgaki K. Structure and stability of ethane hydrate crystal. *Fluid Phase Equilib*. 2000;169:167–175.
69. Hirai H, Takahara N, Kawamura T, Yamamoto Y, Yagi T. Structural changes and preferential cage occupancy of ethane hydrate and methane-ethane mixed gas hydrate under very high pressure. *J Chem Phys*. 2008;129:224503.
70. Domingo C, Montero S. Experimental determination of CH-stretching-bending-bending cubic force-constants of ethane from Raman intensity analysis. *J Chem Phys*. 1987;86:6046–6058.
71. Fernandez JM, Montero S. Torsional selection rules, Raman tensors, and cross sections for degenerate modes of C_2H_6. *J Chem Phys*. 2003;118:2657–2672.
72. Uras-Aytemiz N, Monreal IA, Devlin JP. Communication: Quantitative Fourier-transform infrared data for competitive loading of small cages during all-vapor instantaneous formation of gas-hydrate aerosols. *J Chem Phys*. 2011;135:141103.
73. Falenty A, Kuhs WF. "Self-preservation" of CO_2 gas hydrates-surface microstructure and ice perfection. *J Phys Chem B*. 2009;113:15975–15988.

Manuscript received Aug. 31, 2012, and revision received Nov. 20, 2012.